Research Article | Vol. 31, No. 22 / 23 Oct 2023 / Optics Express 37142
Optics EXPRESS

Manipulating the quasi–normal modes of radially symmetric resonators

JAMES R. CAPERS,[1,*] DEAN A. PATIENT,[1] AND SIMON A. R. HORSLEY[1]

Department of Physics and Astronomy, University of Exeter, Stocker Road, Exeter, EX4 4QL, United Kingdom
[*] *j.capers@exeter.ac.uk*

Abstract: The frequency response of a resonator is governed by the locations of its quasi-normal modes in the complex frequency plane. The real part of the quasi–normal mode determines the resonance frequency and the imaginary part determines the width of the resonance. For applications such as energy harvesting and sensing, the ability to manipulate the frequency, linewidth and multipolar nature of resonances is key. Here, we derive two methods for simultaneously controlling the resonance frequency, linewidth and multipolar nature of the resonances of radially symmetric structures. Firstly, we formulate an eigenvalue problem for a global shift in the permittivity of the structure to place a resonance at a particular complex frequency. Next, we employ quasi-normal mode perturbation theory to design radially graded structures with resonances at desired frequencies.

1. Introduction

Resonances are key to a strong electromagnetic response of photonic components. Over the last two decades resonant interaction has been employed in metamaterials [1–3], nano–antennas [4,5] and super–scatterers [6,7] to almost arbitrarily manipulate electromagnetic radiation. Recently there has been much interest in 'Mietronics' [8,9]. Work in this field has focused on using higher order multipolar modes to achieve greater control of electromagnetic radiation including directional scattering [10], field confinement [11] and frequency selective imaging [12].

Engineering the resonant frequency of any particular multipolar response is crucial for many applications including efficient absorbers [13,14] and thermal emitters for gas sensing [15]. Although the theory of Mie resonances is over 100 years old [16], the problem of designing the spectral response of multipolar resonances remains open.

Many approaches rely on a brute force sweep of the design parameters using memory intensive numerical simulations [17–21] to move resonances, which can be numerically demanding and offers little insight into the final structure. More advanced methods based upon machine learning [22,23] have recently been used to manipulate both electric and magnetic multipole moments, however a large amount of training data must be generated. In addition to this, semi–analytic techniques based upon complex analysis [24] have been developed to enhance the Q–factor of resonances. This exploits the insight provided by the quasi–normal mode framework.

First developed by Gamow to describe alpha decay [25], quasi–normal modes have been employed extensively to model electromagnetic systems in terms of their complex frequency resonances [26–29]. Crucially, for well separated quasi normal mode resonances, the real part of the quasi–normal mode frequency describes the resonance frequency, whereas the imaginary part encodes the spectral width of the resonance. The ability to manipulate the exact location of quasi–normal modes in the complex plane therefore allows one to control the location and width of the resonance simultaneously. Inverse design techniques to manipulate spatial electromagnetic

#503349 https://doi.org/10.1364/OE.503349
Journal © 2023 Received 16 Aug 2023; revised 3 Oct 2023; accepted 8 Oct 2023; published 19 Oct 2023

Optics EXPRESS

responses are well developed [30–33], however few systematic techniques exist to manipulate the spectral response of resonators. In recent years, methods based upon automatic differentiation [34] and shape optimization with quasi–normal mode perturbation theory [35] have been developed to provide a systematic way to manipulate the quasi–normal modes of photonic crystals, however there is still demand for simple and numerically efficient inverse design techniques to solve this problem.

In this work, we develop two techniques to control the spectral location, width, and multipolar nature of the resonances of radially symmetric resonators. Building on previous work that developed a design theory for 1D graded structures [36], we propose a technique to calculate the complex shift one should apply to the permittivity of a resonator to place a particular multipolar resonance at a desired complex frequency. We also employ quasi–normal mode perturbation theory to design graded structures with resonances of specific multipolar character at chosen frequencies. Both techniques are simple, easily extensible and numerically efficient.

2. Finding the quasi–normal modes of radially symmetric resonators

In this section, we briefly review how one can formulate a finite difference scheme to find the quasi–normal modes of a resonator with a radially graded permittivity. Our key results are how these permittivity profiles can be designed, however it will be necessary to find the quasi–normal modes throughout.

The scalar Helmholtz equation governs a wide variety of physical phenomena. For example: pressure acoustics and a single polarisation of the electromagnetic field in 2D, and in 3D it describes the TE polarization of the electromagnetic field [37]. Our work will be a proof–of–concept of our key techniques, however the two methods we will present are easily extended to 3D vector case, as well as to propagating modes in waveguides [38] and other wave regimes such as elasticity [39]. We write the scalar Helmholtz equation as

$$\left[\nabla^2 + k^2\varepsilon(\boldsymbol{r})\right]\psi(\boldsymbol{r}) = 0, \tag{1}$$

describing a single polarisation of the electromagnetic field $\psi(\boldsymbol{r})$ in a material with spatially varying permittivity $\varepsilon(\boldsymbol{r})$ and wavenumber k. Our aim is to find, for a given permittivity profile, the complex eigen–frequencies supported by the structure. Simply re–arranging the Helmholtz Eq. (1), this problem can be formulated as an eigenvalue problem

$$-\frac{1}{\varepsilon}\nabla^2\psi = k^2\psi, \text{subject to } \lim_{r\to\infty} r\left(\frac{\partial}{\partial r} - ik\right)\psi = 0, \tag{2}$$

which includes the radiation boundary condition [40], given in three spatial dimensions. This boundary condition makes the Laplace operator depend upon the eigenvalue k [26,36], meaning that the solution of Eqn. (2) is no longer a straightforward eigenvalue problem [28]. Here, we formulate how this eigenvalue problem can be solved for radially symmetric systems.

For a given radially symmetric permittivity profile $\varepsilon(\boldsymbol{r}) = \varepsilon(r)$ our aim is to find the locations of the quasi–normal modes supported by the resonator. We consider the radially symmetric case for simplicity, however one could employ a topology optimization based approach similar to that in [41] to manipulate resonances arbitrarily. As we are treating radially symmetric resonators, we write the Laplacian in Eqn. (1) in cylindrical or spherical coordinates

$$\nabla^2\psi = \begin{cases} \frac{\partial^2\psi}{\partial r^2} + \frac{1}{r}\frac{\partial\psi}{\partial r} + \frac{1}{r^2}\frac{\partial\psi}{\partial\theta} & \text{2D} \\ \frac{\partial^2\psi}{\partial r^2} + \frac{2}{r}\frac{\partial\psi}{\partial r} + \frac{1}{r^2\sin^2\theta}\frac{\partial\psi}{\partial\theta}\left(\sin\theta\frac{\partial\psi}{\partial\theta}\right) + \frac{1}{r^2\sin^2\theta}\frac{\partial\psi}{\partial\phi} & \text{3D} \end{cases} \tag{3}$$

depending on the number of dimensions we choose to work in. While the calculations are very similar in 2D and 3D, for clarity we proceed with the 3D example providing the 2D calculation in

Optics EXPRESS

the Supplement 1. In the 2D case, we shall consider cylinders with length much longer than the wavelength with polarisation parallel to the long axis, such that the z dimension can be neglected. Separating the angular and radial variables, we write $\psi(\boldsymbol{r}) = \psi(r)Y_\ell^m(\theta,\phi)$, where $Y_\ell^m(\theta,\phi)$ are the spherical harmonics. Substituting this into Eqn. (1) turns the Helmholtz equation into

$$\frac{\partial^2\psi}{\partial r} + \frac{2}{r}\frac{\partial}{\psi}\partial r - \frac{\ell(\ell+1)}{r^2}\psi(r) + k^2\varepsilon(r)\psi(r) = 0. \tag{4}$$

We now remove the first derivative term with the substitution $\psi(r) = \chi(r)/r$, to get

$$\frac{\partial^2\chi}{\partial r^2} - \frac{\ell(\ell+1)}{r^2}\chi + k^2\varepsilon(r)\chi = 0. \tag{5}$$

This has now brought the equation we must solve into the form of the 1D Helmholtz equation, with an additional term related to the angular momentum ℓ. The boundary condition for an outgoing wave that must be imposed is

$$\psi(r\to\infty) = h_\ell^{(1)}(kr), \tag{6}$$

$$\chi(r\to\infty) = rh_\ell^{(1)}(kr), \tag{7}$$

where $h_\ell^{(1)}(kr)$ is the spherical Hankel function of the first kind. Asymptotically, as $kr\to\infty$ the spherical Hankel function goes as $h_\ell^{(1)}(kr)\to i^{-(n+1)}e^{ikr}/(kr)$ [42], clearly satisfying the radiation boundary condition. This means that the boundary condition upon the derivative of the field can be written as

$$\frac{\partial\chi}{\partial r} = h_\ell^{(1)}(kr)\left[1 + (kr)\frac{h_\ell^{(1)\prime}(kr)}{h_\ell^{(1)}(kr)}\right] \tag{8}$$

$$= \chi(r)\left[\frac{1}{r} + k\frac{h_\ell^{(1)\prime}(kr)}{h_\ell^{(1)}(kr)}\right] \tag{9}$$

$$= \chi\gamma(k). \tag{10}$$

To impose this boundary condition, we shall need to modify the finite difference matrix that will numerically represent the Laplacian operator. We therefore write the boundary condition given by Eqn. (10) in forwards finite difference form

$$\chi_{n+1} = \chi_n(1 + \Delta r\gamma(k)). \tag{11}$$

At this point, the boundary condition corresponding to quasi–normal modes can be imposed on the Laplacian. However, to find the modes we must remove the dependence upon k from the finite difference Laplacian matrix. This can be achieved by linearising $\gamma(k)$ around a particular frequency $k_\star$, giving

$$\gamma(k) = \gamma(k_\star) + (k-k_\star)\partial_k\gamma(k_\star) = A + kB, \tag{12}$$

where $A = \gamma(k_\star) - k_\star\partial_k\gamma(k_\star)$ and $B = \partial_k\gamma(k_\star)$. This is an approximation that allows us to separate the eigen–value from the boundary condition, which is necessary to formulate the eigen–value problem. If the value around which one expands $k_\star$ is far from the eigen–value k then this method will fail to find the correct eigen–value. This is an issue common to many numerical techniques used to solve eigenvalue problems. One could in principle expand to quadratic or cubic terms to improve the quality of the approximation, however this would increase the size

Optics EXPRESS

of the resulting eigen–value problem. We can now formulate the eigenvalue problem posed by Eqn. (2) such that the eigenvalue k only appears on the right–hand side. Defining

$$\mathcal{L} = \frac{1}{\Delta r^2}\begin{pmatrix} -2 & 1 & 0 & \cdots & 0 \\ 1 & -2 & 1 & \cdots & 0 \\ 0 & 1 & -2 & \cdots & 0 \\ \vdots & \vdots & \vdots & \ddots & \vdots \\ 0 & 0 & 0 & \cdots & (A\Delta r - 1) \end{pmatrix}, \quad \mathcal{L}' = \frac{1}{\Delta r^2}\begin{pmatrix} 0 & 0 & 0 & \cdots & 0 \\ 0 & 0 & 0 & \cdots & 0 \\ 0 & 0 & 0 & \cdots & 0 \\ \vdots & \vdots & \vdots & \ddots & \vdots \\ 0 & 0 & 0 & \cdots & B\Delta r \end{pmatrix}. \tag{13}$$

we can split the Helmholtz equation into

$$\left(\mathcal{L} + k\mathcal{L}' - \frac{\ell(\ell+1)}{r^2} + k^2\varepsilon(r)\right)\chi = 0. \tag{14}$$

This can then be formed into a quadratic eigenvalue problem [43]

$$\begin{pmatrix} \mathbf{0} & \mathbf{1} \\ -(\mathcal{L} - \ell(\ell+1)/r^2)/\varepsilon(r) & -\mathcal{L}'/\varepsilon(r) \end{pmatrix}\begin{pmatrix} \chi \\ k\chi \end{pmatrix} = k\begin{pmatrix} \chi \\ k\chi \end{pmatrix}. \tag{15}$$

While the first of these two equations is trivial, it is necessary to introduce it so that χ and $k\chi$ terms can be coupled. For radially graded structures, this gives both the radial part of the field of the mode and the eigenfrequency k.

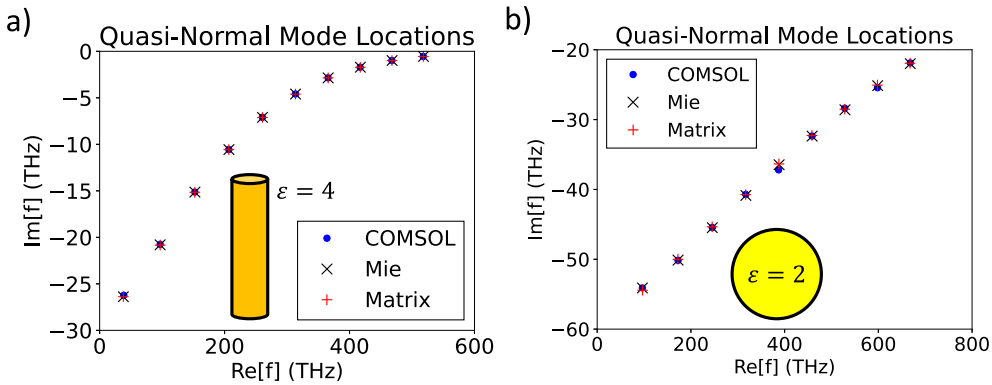

Fig. 1. A comparison of different methods for finding the quasi–normal modes of isotropic cylinders or spheres. The method labelled 'matrix' indicates the finite difference implementation we have developed in Section 2. a) shows the comparison for a cylinder, and b) for a sphere. Both the cylinder and the sphere have radius $a = 550$ nm.

To verify this method, we compare it to other methods for finding quasi–normal modes. For isotropic cylinders and spheres, Mie theory can be used to find the complex frequencies analytically. Full–wave solvers such as COMSOL Multiphysics [44] can be employed to find the complex eigenfrequencies of spatially varying structures. Both COMSOL and the method we have outlined here require frequencies to search around, so one must already have an idea of roughly where the resonance is located. Fig. 1 shows the comparison of the three methods of finding the quasi–normal mode frequencies of isotropic cylinders and spheres. We have chosen the cylinder and sphere to have radius $a = 550$ nm, with the cylinder having a permittivity of $\varepsilon = 4$ and the sphere $\varepsilon = 2$. Details of the Mie theory are given in Supplement 1.[!t]

Optics EXPRESS

With a method of finding both the complex frequency and mode profile of the quasi-normal modes of cylinders and spheres, we proceed to consider two methods for engineering the permittivity such that resonances are placed at particular complex frequencies. This allows one to achieve a high level of control over the spectral response of a scatterer. The methods we shall present can be used to move any multipolar resonance to any complex frequency, regardless of how closely the modes are spaced. To illustrate the versatility of our method, in the following sections we arbitrarily choose particular multipolar resonances, characterised by their angular momentum ℓ, to be moved to particular target frequencies.

3. Moving resonances by finding permittivity shifts

As outlined in the previous section, finding quasi–normal modes can result in large eigen–value problems. While it is often useful to decompose the response of a resonator into a sum over the quasi–normal modes many issues arise from questions over normalisation and completeness of the basis set [29,45]. To address this, it was noted that one could instead form 'eigen–permittivity' modes, where the eigen–value is the permittivity rather than the wave–number [46–49]. Such modes are normalizable and form a complete basis, making them extremely useful when analysing scattering problems [50,51] or decomposing the response of emitters to a structured photonic environment [52]. These methods also benefit from related asymptotic techniques [53–55]. Unlike this previous work, we treat the permittivity of the resonator as a complex–valued parameter that can be tuned to achieve resonance at a desired complex frequency. To this end, we split the permittivity into a spatially varying part $\varepsilon(r)$ and a background shift ε_b, that is applied only to the resonator (not the free–space surrounding it). This allows us to rearrange the Helmholtz Eq. (1) into an eigenvalue problem for the background permittivity

$$\left[\nabla^2 + k^2(\varepsilon(r) + \varepsilon_b)\right]\phi = 0, \tag{16}$$

$$-\frac{1}{k^2}\left[\nabla^2 + k^2\varepsilon(r)\right]\phi = \varepsilon_b\phi. \tag{17}$$

To use this, one can choose a complex k at which one wants the quasi–normal mode to occur, then solve the eigenvalue problem to find the corresponding (complex) permittivity shift ε_b. Unlike previous results [36], for radially symmetric resonators the Laplacian contains information about the angular momentum of the mode that is placed at the desired k. One can therefore control both the spectral properties and the multipolar nature of the resonance simultaneously. It is important to note that in order to solve the eigenvalue problem posed by Eqn. (17), the finite difference Laplacian operator must be modified to have the outgoing wave boundary condition at the edge of the resonator, as was discussed in Section 2..

An example of this procedure for a cylinder is shown in Fig. 2. Starting from an isotropic cylinder of radius $a = 550$ nm and permittivity $\varepsilon = 4$, the $\ell = 3$ resonance is initially at $f \sim 200 - i10$ THz. We seek to move this to $f = 150 - i2$ THz, corresponding to a lower resonance frequency and smaller linewidth, giving a background shift of $\varepsilon_b = 4.15 + i0.007$. Applying this, we find the $\ell = 3$ mode at the desired frequency. To verify this, full–wave simulations are employed to calculate the scattered energy from the cylinder. These simulations were performed in COMSOL Multiphysics [44], using the scattered field formulation. Exciting with a background plane wave, the scattered power was obtained by integrating power outflow over the outer boundary of the simulation. This integral, as a function of frequency, is what is reported in the figures. While gain can be introduced to the scatterer if the permittivity shift has $\mathrm{Im}[\varepsilon_b]<0$, this is limited to the resonator itself. It is well–known that the spectral response of a resonator with several well spaced quasi–normal modes can be approximated as a series of Lorentzians [26], with the peak locations corresponding to the real part of the quasi–normal modes and the widths corresponding to the imaginary parts. Thus, to verify that moving the

Optics EXPRESS

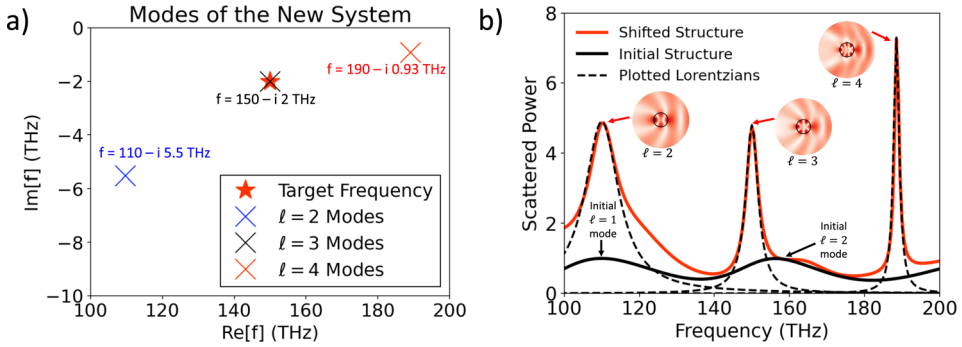

Fig. 2. Using the permittivity–shift method to place the $\ell = 3$ mode of an isotropic cylinder. We seek to move the $\ell = 3$ mode to 150-i2 THz, requiring a permittivity shift of $\varepsilon_b = 4.15 + i0.007$. a) The locations of the quasi–normal modes. b) Full–wave simulations verifying the scattering behaviour of the cylinder. Peak locations and widths can be related directly to pole locations, and the fields $|\psi|$ shown inset verify the multipolar nature of the modes. As the inset plots are of the field norm, the $\ell = 3$ lobe should exhibit 6 amplitude peaks. For comparison, the spectra of the un–shifted resonator is shown.

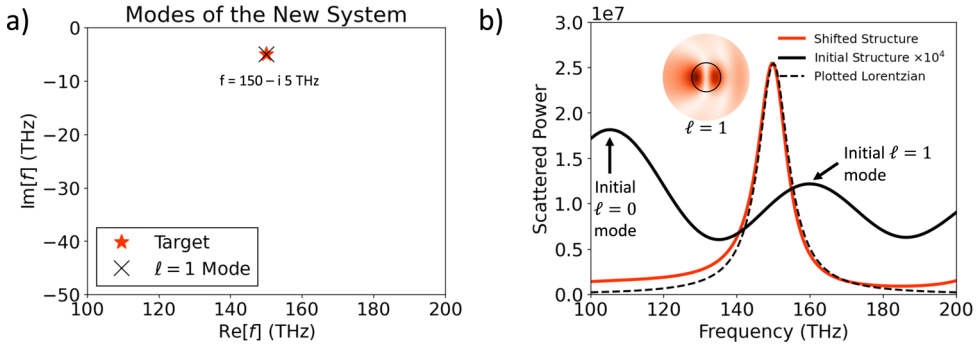

Fig. 3. Finding a permittivity shift to place the dipole $\ell = 1$ mode of an isotropic sphere at $f = 150 - i5$ THz. A background permittivity shift of $\varepsilon_b = 0.96 - i0.88$. Locations of the modes are shown in a). b) Scattered power is then calculated using full–wave simulations, with the mode profile at 150 THz shown inset. The spectra of the un–shifted sphere is shown in black for comparison.

resonances has had the desired effect on the scattering from the resonator, we plot Lorentzians of the form

$$L(f, f_0, \Gamma) = A\frac{\Gamma}{(f - f_0)^2 + \Gamma^2} \tag{18}$$

over the scattered power data. In some cases, slightly different functions might be a better fit [56] however this requires detailed analysis. Throughout, the central frequency f_0 is taken from the real part of the mode with the width Γ corresponding to the expected imaginary part and A is the amplitude scale. At $f = 150$ THz there is a peak corresponding to the $\ell = 3$ quasi–normal mode, with a width corresponding to the imaginary part of the quasi–normal mode frequency. Examining the field profile of the resonator, shown inset, we observe that the multipolar nature of the mode is as expected. Other peaks in the spectrum are explained by the presence of the $\ell = 2$ and $\ell = 4$ modes in the vicinity of the mode we have moved.

We also apply this method to move the $\ell = 1$ dipole mode of a sphere of initial permittivity $\varepsilon = 2$. The dipole mode is chosen as it has been utilised extensively to enable dielectric

Optics EXPRESS

metamaterials to interact strongly with light [57]. Initially, this mode is located at $f = 172 + i50$ THz. Setting the target frequency to be $f = 150 - i5$ THz, corresponding to a lower resonance frequency and 10 times smaller linewidth, we solve the eigenvalue problem posed by Eqn. (17) to obtain a permittivity offset of $\varepsilon_b = 0.96 - i0.88$. The modes of the new system, as well as the scattered power are shown in Fig. 3. Due to the gain that has been added to the resonator, there is a significant increase in the scattered power.

4. Moving Resonances by radially grading the permittivity

The next method we propose employs a radial grading of the permittivity to provide control over the spectral location of the quasi–normal modes of a resonator. For this design strategy we employ perturbation theory to connect a small change in the structure to a small change in the position of a quasi–normal mode. Applying perturbation theory to quasi–normal modes is challenging as the modes grow in space and so cannot be trivially normalised [45]. Originally developed by Zel'Dovich [58], quasi–normal mode perturbation theory has been greatly developed over the last 6 decades [59–62], with various regularization techniques being developed. This has led to the application of quasi–normal mode perturbation theory to a wide range of systems including planar structures [63], waveguides [64] and graded index spheres [37]. While most works to date have focused on the development of quasi–normal mode perturbation theory, we use it to enable an automated design procedure. Seeking to grade spherically symmetric resonators in a way that moves a resonance to a desired location, we note that small change in the permittivity of the the resonator $\delta\varepsilon(r)$ is connected to a change in the position of the quasi–normal mode by the following expression [59,60]

$$\delta k_n = -\frac{k_n}{2}\frac{\int_0^a dr\psi_n^2(r)\delta\varepsilon(r)}{\int_0^a \psi_n^2\varepsilon(r)dr + \frac{i}{2k_n}\psi_n^2(a)}, \tag{19}$$

where a is the radius of the resonator and $\psi_n(r)$ is the field profile associated with the mode. While there is much discussion in the literature about how to normalise quasi–normal modes [65], Eq. (19) is a natural consequence of applying perturbation to the wave–equation. We consider only perturbations to the resonator itself, not to the surrounding environment as in [66]. Re-writing the normalisation factor on the denominator as $\langle\psi_n|\psi_n\rangle$ and changing the permittivity at a single point r_i so that $\delta\varepsilon(r) = \Delta\varepsilon\delta(r - r_i)$, we find that the gradient of the location of the quasi–normal mode with respect to the permittivity is

$$\frac{\partial k_n}{\partial\varepsilon} = -\frac{k_n}{2}\frac{\psi_n^2(r)}{\langle\psi_n|\psi_n\rangle}. \tag{20}$$

For quasi–normal modes, the norm $\langle\psi_n|\psi_n\rangle$ now contains additional boundary terms due to the out–going wave boundary condition imposed at the edge of the system.

Now, say we would like to place a particular mode at a given complex frequency k_{target}. Defining the figure of merit as

$$\mathcal{F} = (k_n - k_{\text{target}})^2, \tag{21}$$

we find that the gradient of the figure of merit with respect to the permittivity is

$$\frac{\partial\mathcal{F}}{\partial\varepsilon} = (k_n - k_{\text{target}})\frac{\partial k_n}{\partial\varepsilon} \tag{22}$$

$$= -\frac{k_n}{2}(k_n - k_{\text{target}})\frac{\psi_n^2(r)}{\langle\psi_n|\psi_n\rangle}. \tag{23}$$

This result is key: we have an analytic expression for how to change the permittivity at every radial position in order to minimise (or maximise) our chosen figure of merit. Like the adjoint

Optics EXPRESS

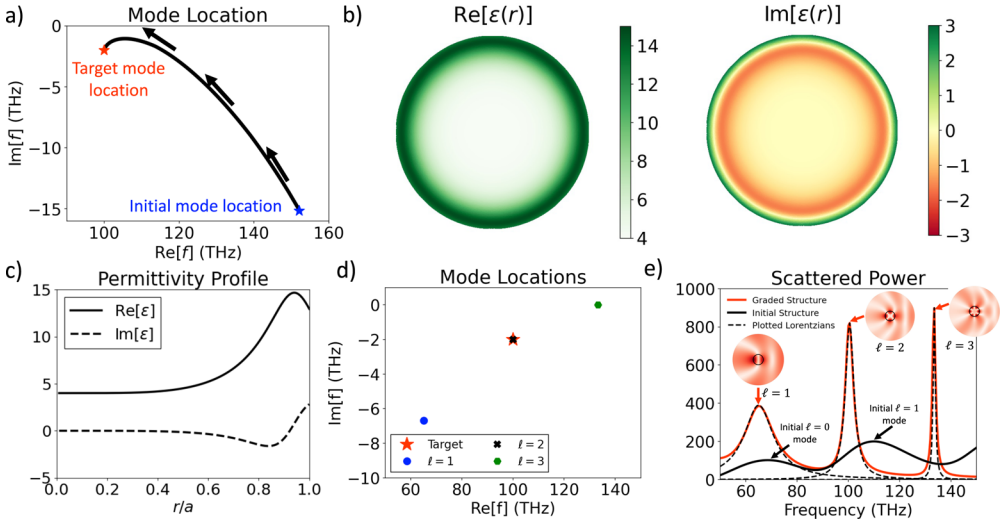

Fig. 4. Designing a graded cylinder with a quadrupole resonance at 100-i2 THz. a) The iterative movement of the $\ell = 2$ mode from 152-i15 THz to the desired complex frequency of 100 - i2 THz. Panels b) and c) show the resulting permittivity distribution, which has the modes shown in d). e) Full–wave simulations of the scattered power indicate peaks corresponding to each pole, with inset electric fields show that each mode exhibits the expected multipolar nature. The power scattered by the un–graded cylinder is given for comparison.

method for designing graded wave–shaping devices [31,67,68], this provides a numerically efficient tool for designing graded structures. In this case, we can design graded cylinders or spheres with specified complex quasi–normal mode frequencies with a chosen multipolar character. As quasi–normal mode perturbation theory is only used to find how to change the structure, this approach remains valid for systems with many nearby resonances, although one might have to update the permittivity profile in smaller steps. The key limitation of this method is that in its current implementation, only a single mode can be manipulated at a time.

This method is demonstrated in Fig. 4. Starting from an isotropic cylinder of permittivity $\varepsilon = 4$, the mode locations k_n and fields ψ_n are found using the matrix formulation presented in Section 2.. Choosing to move the $\ell = 2$ mode from $f \sim 250 - i45$ THz to $f_{\text{target}} = 100 - i2$ THz, the figure of merit we seek to optimise is defined by Eqn. (21). Evaluating the gradient of the figure of merit according to Eqn. (23), the permittivity profile is iteratively updated using gradient descent [69]

$$\varepsilon^{i+1}(r) = \varepsilon^{i}(r) + \gamma \frac{\partial \mathcal{F}}{\partial \varepsilon^{i}}, \tag{24}$$

where the index i indicates the iteration number. This expression allows for the entire profile to be updated each step. The progress of the optimisation is shown in Fig. 4(a), where the mode moves through the complex plane as the structure is updated. The designed permittivity grading is shown in Fig. 4(b) and (c), with the mode locations of the structure shown in panel d). We note that in order to move the quasi–normal mode towards the real frequency axis one must introduce gain, indicated by Im[ε]<0. To verify that the mode has been moved, power scattered from the graded structure has been calculated with finite element full–wave simulations using COMSOL Multiphysics [44], with the field distributions associated with each peak shown inset. A Lorentzian is plotted in Fig. 4(e) with a width and central frequency corresponding to the desired location of the quasi–normal mode in the complex plane. Next, we consider grading the

Optics EXPRESS

permittivity of an initially isotropic sphere of permittivity $\varepsilon = 2$ to move the $\ell = 4$ resonance to $f_{\text{target}} = 250 - i5$ THz. Using the same framework, the progression of the optimisation is shown in Fig. 5(a), with the designed permittivity profile shown in Fig. 5(b). The locations of the new modes as well as the scattered power, calculated using full–wave simulations, is shown in Fig. 5(c) and (d) respectively. In both examples, one can note that most of the grading occurs at distance r/a>0.6. This is because we are working with modes that vanish at the center of the resonator and manipulating the permittivity in the region where the field is larger gives greater control over the mode location. One interesting way this approach might be extended is to consider shape deformations, rather than permittivity changes, of the radially symmetric resonator. Perturbation theory for shape changes to a resonator was developed around around a few decades ago [70,71] and has garnered recent interest for the nearly spherical resonators [72–74]. Coupled with this framework, our approaches might be used to facilitate the inverse design of non–spherical resonators.

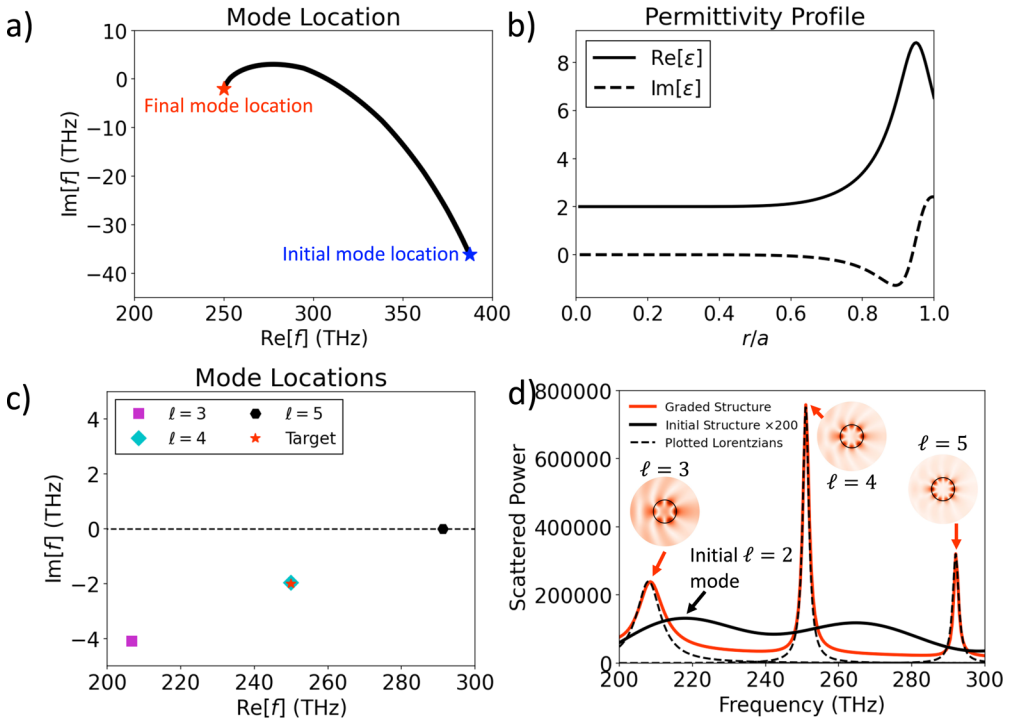

Fig. 5. Design of a graded sphere with a $\ell = 4$ resonance at 250 - i5 THz. a) Progression of the mode over the iterative optimisation, giving b) the final radial permittivity grading. c) Mode locations of the final graded sphere correspond directly to peaks in the d) scattered power. The power scattered by the un–graded sphere is shown for comparison. Electric field profiles associated with each mode are shown inset.

5. Conclusion

We have developed two techniques to solve the problem of designing cylindrical and spherical resonators with multipolar resonances at desired complex frequencies. The first approach involves formulating an eigenvalue problem for a complex permittivity shift of the resonator so that a given mode is placed at a particular location. The second method uses quasi–normal mode perturbation theory to establish a connection between a small change in the permittivity distribution and a small

Optics EXPRESS

change in the location of a quasi–normal mode. This is then used to form an analytic expression for the gradient of a figure of merit, taken to be the difference between the location of the mode and a desired location. With this, the permittivity distribution of the resonator is iteratively updated until the mode is at the desired spectral location. These methods have the benefit of controlling the resonance frequency of the mode, its linewidth and multipolar nature simultaneously. While our results are, at this point, purely proof–of–concept, to apply these to more practical designs, one could employ a purely numerical approach. The eigen–value problem for the permittivity shift could be set up in numerical solvers such as COMSOL, which could also be used to find the mode fields used to update the structure in the grading technique. In this way, one could design realistic scatterers, perhaps with stratified permittivity profiles. Additionally, the ability to design structures with very narrow resonances is useful for building frequency multiplexed devices. We expect our methods to find utility in a range of problems from metamaterial design and sensing to optical computing and communication. Future developments of our methods might involve including the effects of material dispersion as well as manipulating multiple modes simultaneously. The ability to arrange the several resonances at desired frequencies would be useful in the design of super–scatterers. In addition, control over the polarisation of the scattered mode might allow the design of sensors that are polarisation dependent or enable metasurface functionality to be multiplexed.

Funding. Royal Society (URF\R\211033); Engineering and Physical Sciences Research Council (EP/L015331/1); Defence Science and Technology Laboratory.

Acknowledgments. J.R.C. would like to thank Josh G. Glasbey and Dr. Ian R. Hooper for many useful discussions.

Disclosures. The author declare no conflicts of interest.

Data availability. All data and code created during this research are openly available from the corresponding authors, upon reasonable request.

Supplemental document. See Supplement 1 for supporting content.

References

1. B. A. Munk, Frequency Selective Surfaces: Theory and Design (John Wiley and Sons, New York, 2000).
2. I. Staude, A. E. Miroshnichenko, M. Decker, N. T. Fofang, S. Liu, E. Gonzales, J. Dominguez, T. S. Luk, D. N. Neshev, I. Brener, and Y. Kivshar, "Tailoring directional scattering through magnetic and electric resonances in subwavelength silicon nanodisks," ACS Nano **7**(9), 7824–7832 (2013).
3. M. Hentschel, K. Koshelev, F. Sterl, S. Both, J. Karst, L. Shamsafar, T. Weiss, Y. Kivshar, and H. Giessen, "Dielectric mie voids: confining light in air," Light: Sci. Appl. **12**(1), 3 (2023).
4. L. Novotny and N. van Hulst, "Antennas for light," Nat. Photonics **5**(2), 83–90 (2011).
5. P. Bharadwaj, B. Deutsch, and L. Novotny, "Optical antennas," Adv. Opt. Photonics **1**(3), 438 (2009).
6. A. W. Powell, J. Ware, J. G. Beadle, D. Cheadle, T. H. Loh, A. P. Hibbins, and J. R. Sambles, "Strong, omnidirectional radar backscatter from subwavelength, 3d printed metacubes," IET Microw. **14**, 1862–1868 (2020).
7. E. D. Finlayson, C. P. Gallagher, T. Whittaker, A. Goulas, D. S. Engstrøm, W. Whittow, J. R. Sambles, A. P. Hibbins, and A. W. Powell, "Microwave backscatter enhancement using radial anisotropy in biomimetic core-shell spheres," Appl. Phys. Lett. **122**(25), 251701 (2023).
8. R. Won, "Into the 'mie-tronic' era," Nat. Photonics **13**(9), 585–587 (2019).
9. K. Koshelev and Y. Kivshar, "Dielectric resonant metaphotonics," ACS Photonics **8**(1), 102–112 (2021).
10. Y. H. Fu, A. I. Kuznetsov, A. E. Miroshnichenko, Y. F. Yu, and B. Luk'yanchuk, "Directional visible light scattering by silicon nanoparticles," Nat. Commun. **4**(1), 1527 (2013).
11. A. E. Miroshnichenko, A. B. Evlyukhin, Y. F. Yu, R. M. Bakker, A. Chipouline, A. I. Kuznetsov, B. Luk'yanchuk, B. N. Chichkov, and Y. S. Kivshar, "Nonradiating anapole modes in dielectric nanoparticles," Nat. Commun. **6**(1), 8069 (2015).
12. A. Tittl, A. Leitis, M. Liu, F. Yesilkoy, D.-Y. Choi, D. N. Neshev, Y. S. Kivshar, and H. Altug, "Imaging-based molecular barcoding with pixelated dielectric metasurfaces," Science **360**(6393), 1105–1109 (2018).
13. K. Aydin, V. E. Ferry, R. M. Briggs, and H. A. Atwater, "Broadband polarization-independent resonant light absorption using ultrathin plasmonic super absorbers," Nat. Commun. **2**(1), 517 (2011).
14. N. I. Landy, S. Sajuyigbe, J. J. Mock, D. R. Smith, and W. J. Padilla, "Perfect metamaterial absorber," Phys. Rev. Lett. **100**(20), 207402 (2008).
15. A. Lochbaum, Y. Fedoryshyn, A. Dorodnyy, U. Koch, C. Hafner, and J. Leuthold, "On-chip narrowband thermal emitter for mid-ir optical gas sensing," ACS Photonics **4**(6), 1371–1380 (2017).
16. G. Mie, "Beiträge zur optik trüber medien, speziell kolloidaler metallösungen," Ann. Phys. **330**(3), 377–445 (1908).

Optics EXPRESS

17. V. Grigoriev, A. Tahri, S. Varault, B. Rolly, B. Stout, J. Wenger, and N. Bonod, "Optimization of resonant effects in nanostructures via weierstrass factorization," Phys. Rev. A **88**(1), 011803 (2013).
18. T. Wu, A. Baron, P. Lalanne, and K. Vynck, "Intrinsic multipolar contents of nanoresonators for tailored scattering," Phys. Rev. A **101**(1), 011803 (2020).
19. J. van de Groep and A. Polman, "Designing dielectric resonators on substrates: Combining magnetic and electric resonances," Opt. Express **21**(22), 26285–26302 (2013).
20. C. Gigli, T. Wu, G. Marino, A. Borne, G. Leo, and P. Lalanne, "Quasinormal-mode non-hermitian modeling and design in nonlinear nano-optics," ACS Photonics **7**(5), 1197–1205 (2020).
21. N. Granchi, M. Montanari, A. Ristori, M. Khoury, M. Bouabdellaoui, C. Barri, L. Fagiani, M. Gurioli, M. Bollani, M. Abbarchi, and F. Intonti, "Near-field hyper-spectral imaging of resonant mie modes in a dielectric island," APL Photonics **6**(12), 126102 (2021).
22. A. Estrada-Real, A. Khaireh-Walieh, B. Urbaszek, and P. R. Wiecha, "Inverse design with flexible design targets via deep learning: Tailoring of electric and magnetic multipole scattering from nano-spheres," Photonics Nanostructures: Fundam. Appl. **52**, 101066 (2022).
23. W. Li, H. B. Sedeh, W. J. Padilla, S. Ren, J. Malof, and N. M. Litchinitser, "Machine learning for mie-tronics," arXiv, arXiv:2305.18589v1 (2023).
24. F. Binkowski, F. Betz, M. Hammerschmidt, P.-I. Schneider, L. Zschiedrich, and S. Burger, "Computation of eigenfrequency sensitivities using riesz projections for efficient optimization of nanophotonic resonators," Commun. Phys. **5**(1), 202 (2022).
25. G. Gamow, "Zur quantentheorie des atomkernes," Z. Physik **51**(3-4), 204–212 (1928).
26. P. T. Kristensen, K. Herrmann, F. Intravaia, and K. Busch, "Modeling electromagnetic resonators using quasinormal modes," Adv. Opt. Photonics **12**(3), 612–708 (2020).
27. R.-C. Ge, P. T. Kristensen, J. F. Young, and S. Hughes, "Quasinormal mode approach to modelling light-emission and propagation in nanoplasmonics," New J. Phys. **16**(11), 113048 (2014).
28. P. Lalanne, W. Yan, A. Gras, C. Sauvan, J.-P. Hugonin, M. Besbes, G. Demésy, M. D. Truong, B. Gralak, F. Zolla, A. Nicolet, F. Binkowski, L. Zschiedrich, S. Burger, J. Zimmerling, R. Remis, P. Urbach, H. T. Liu, and T. Weiss, "Quasinormal mode solvers for resonators with dispersive materials," J. Opt. Soc. Am. A **36**(4), 686–704 (2019).
29. P. Lalanne, W. Yan, K. Vynck, C. Sauvan, and J.-P. Hugonin, "Light interaction with photonic and plasmonic resonances," Laser Photonics Rev. **12**(5), 1700113 (2018).
30. S. Molesky, Z. Lin, A. Y. Piggott, W. Jin, J. Vuckovic, and A. W. Rodriguez, "Inverse design in nanophotonics," Nat. Photonics **12**(11), 659–670 (2018).
31. C. M. Lalau-Keraly, S. Bhargava, O. D. Miller, and E. Yablonovitch, "Adjoint shape optimization applied to electromagnetic design," Opt. Express **21**(18), 21693–21701 (2013).
32. J. R. Capers, S. J. Boyes, A. P. Hibbins, and S. A. R. Horsley, "Designing the collective non-local responses of metasurfaces," Commun. Phys. **4**(1), 209 (2021).
33. J. R. Capers, S. J. Boyes, A. P. Hibbins, and S. A. R. Horsley, "Designing disordered multi-functional metamaterials using the discrete dipole approximation," New J. Phys. **24**(11), 113035 (2022).
34. M. Minkov, I. A. D. Williamson, L. C. Andreani, D. Gerace, B. Lou, A. Y. Song, T. W. Hughes, and S. Fan, "Inverse design of photonic crystals through automatic differentiation," ACS Photonics **7**(7), 1729–1741 (2020).
35. N. Granchi, F. Intonti, M. Florescu, P. D. García, M. Gurioli, and G. Arregui, "Q factor optimization of modes in ordered and disordered photonic systems using non-hermitian perturbation theory," ACS Photonics **10**(8), 2808–2815 (2023).
36. J. R. Capers, D. A. Patient, and S. A. R. Horsley, "Inverse design in the complex plane: Manipulating quasinormal modes," Phys. Rev. A **106**(5), 053523 (2022).
37. Z. Sztranyovszky, W. Langbein, and E. A. Muljarov, "Optical resonances in graded index spheres: A resonant-state-expansion study and analytic approximations," Phys. Rev. A **105**(3), 033522 (2022).
38. S. Upendar, I. Allayarov, M. A. Schmidt, and T. Weiss, "Analytical mode normalization and resonant state expansion for bound and leaky modes in optical fibers - an efficient tool to model transverse disorder," Opt. Express **26**(17), 22536–22546 (2018).
39. A.-L. El-Sayed and S. Hughes, "Quasi-normal mode theory of elastic purcell factors and fano resonances in optomechanical beams," Phys. Rev. Res. **2**(4), 043290 (2020).
40. A. Sommerfeld, Partial Differential Equations in Physics (Academic Press, 1949).
41. H. Goh and A. Alú, "Nonlocal scatterer for compact wave-based analog computing," Phys. Rev. Lett. **128**(7), 073201 (2022).
42. "*NIST Digital Library of Mathematical Functions*," Release 1.1.10 of 2023-06-15, https://dlmf.nist.gov/ F. W. J. Olver, A. B. Olde Daalhuis, D. W. Lozier, B. I. Schneider, R. F. Boisvert, C. W. Clark, B. R. Miller, B. V. Saunders, H. S. Cohl, and M. A. McClain, eds.
43. F. Tisseur and K. Meerbergen, "The quadratic eigenvalue problem," SIAM Rev. **43**(2), 235–286 (2001).
44. "COMSOL® www.comsol.com Multiphysics v. 6.1," COMSOL AB, Stockholm, Sweden.
45. P. L. C. Sauvan, T. Wu, R. Zarouf, and E. A. Muljarov, "Normalization, orthogonality and completeness of quasinormal modes of open systems: the case of electromagnetism," Opt. Express **30**(5), 6846–6885 (2022).
46. D. J. Bergman, "Dielectric constant of a two-component granular composite: A practical scheme for calculating the pole spectrum," Phys. Rev. B **19**(4), 2359–2368 (1979).

Optics EXPRESS

47. D. J. Bergman, "The dielectric constant of a simple cubic array of identical spheres," J. Phys. C: Solid State Phys. **12**(22), 4947–4960 (1979).
48. D. J. Bergman and D. Stroud, "Theory of resonances in the electromagnetic scattering by macroscopic bodies," Phys. Rev. B **22**(8), 3527–3539 (1980).
49. M. S. Agranovich, B. Z. Katsenelenbaum, A. N. Sivov, and N. N. Voitovich, Generalized Method of Eigenoscillations in Diffraction Theory (Wiley-VCH, Berlin, New York, 1999).
50. C. Forestiere and G. Miano, "Material-independent modes for electromagnetic scattering," Phys. Rev. B **94**(20), 201406 (2016).
51. C. Forestiere, G. Miano, G. Rubinacci, A. Tamburrino, R. Tricarico, and S. Ventre, "Volume integral formulation for the calculation of material independent modes of dielectric scatterers," IEEE Trans. Antennas Propag. **66**(5), 2505–2514 (2018).
52. P. Y. Chen, D. J. Bergman, and Y. Sivan, "Generalizing normal mode expansion of electromagnetic green's tensor to open systems," Phys. Rev. Appl. **11**(4), 044018 (2019).
53. O. Schnitzer, "Singular perturbations approach to localized surface-plasmon resonance: nearly touching metal nanospheres," Phys. Rev. B **92**(23), 235428 (2015).
54. O. Schnitzer, "Asymptotic approximations for the plasmon resonances of nearly touching spheres," Eur. J. Appl. Math. **31**(2), 246–276 (2020).
55. O. Schnitzer, "Plasmonic resonances of slender nanometallic rings," Phys. Rev. B **105**(12), 125412 (2022).
56. C. Sauvan, J. P. Hugonin, I. S. Maksymov, and P. Lalanne, "Theory of the spontaneous optical emission of nanosize photonic and plasmon resonators," Phys. Rev. Lett. **110**(23), 237401 (2013).
57. I. Staude and J. Schilling, "Metamaterial-inspired silicon nanophotonics," Nat. Photon. **11**(5), 274–284 (2017).
58. Y. B. Zel'Dovich, "On the theory of unstable states," Nat. Photonics **12**, 3 (1961).
59. P. T. Leung, S. Y. Liu, and K. Young, "Completeness and orthogonality of qnasinormal modes in leaky optical cavities," Phys. Rev. A **49**(4), 3057–3067 (1994).
60. P. T. Leung, S. Y. Liu, and K. Young, "Completeness and time-independent perturbation of the quasinormal modes of an absorptive and leaky cavity," Phys. Rev. A **49**(5), 3982–3989 (1994).
61. P. T. Leung, Y. T. Liu, W. M. Suen, C. Y. Tam, and K. Young, "Logarithmic perturbation theory for quasinormal modes," J. Phys. A: Math. Gen. **31**(14), 3271–3286 (1998).
62. E. A. Muljarov, W. Langbein, and R. Zimmermann, "Brillouin-wigner perturbation theory in open electromagnetic systems," EPL **92**(5), 50010 (2010).
63. M. B. Doost, W. Langbein, and E. A. Muljarov, "Resonant-state expansion applied to planar open optical systems," Phys. Rev. A **85**(2), 023835 (2012).
64. S. V. Lobanov, G. Zoriniants, W. Langbein, and E. A. Muljarov, "Resonant-state expansion of light propagation in nonuniform waveguides," Phys. Rev. A **95**(5), 053848 (2017).
65. P. T. Kristensen, R.-C. Ge, and S. Hughes, "Normalization of quasinormal modes in leaky optical cavities and plasmonic resonators," Phys. Rev. A **92**(5), 053810 (2015).
66. D. J. Bergman, "Eigenstates of maxwell's equations in multiconstituent microstructures," Phys. Rev. A **105**(6), 062213 (2022).
67. A. Y. Piggott, J. Lu, K. G. Lagoudakis, J. Petykiewicz, T. M. Babinec, and J. Vuckovic, "Inverse design and demonstration of a compact and broadband on-chip wavelength demultiplexer," Nat. Photonics **9**(6), 374–377 (2015).
68. J. R. Capers, "Inverse design of thin-plate elastic wave devices," Phys. Rev. Appl. **20**(3), 034064 (2023).
69. S. Shalev-Shwartz and S. Ben-David, Understanding Machine Learning: From Theory to Algorithms (Cambridge University Press, 2014).
70. H. M. Lai, P. T. Leung, K. Young, P. W. Barber, and S. C. Hill, "Time-independent perturbation for leaking electromagnetic modes in open systems with application to resonances in microdroplets," Phys. Rev. A **41**(9), 5187–5198 (1990).
71. S. G. Johnson, M. Ibanescu, M. A. Skorobogatiy, O. Weisberg, J. D. Joannopoulos, and Y. Fink, "Perturbation theory for maxwell's equations with shifting material boundaries," Phys. Rev. E **65**(6), 066611 (2002).
72. A. Aiello, J. G. E. Harris, and F. Marquardt, "Perturbation theory of optical resonances of deformed dielectric spheres," Phys. Rev. A **100**(2), 023837 (2019).
73. W. Yan, P. Lalanne, and M. Qiu, "Shape deformation of nanoresonator: A quasinormal-mode perturbation theory," Phys. Rev. Lett. **125**(1), 013901 (2020).
74. J. Gohsrich, T. Shah, and A. Aiello, "Perturbation theory of nearly spherical dielectric optical resonators," Phys. Rev. A **104**(2), 023516 (2021).